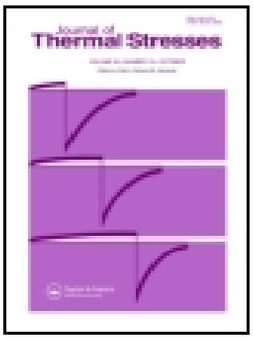

Journal of Thermal Stresses

ISSN: (Print) (Online) Journal homepage: https://www.tandfonline.com/loi/uths20

On Kjartansson model of thermoelastic attenuation

José M. Carcione, Faisal Alonaizi, Ayman N. Qadrouh, Mamdoh Alajmi & Jing Ba

To cite this article: José M. Carcione, Faisal Alonaizi, Ayman N. Qadrouh, Mamdoh Alajmi & Jing Ba (2023): On Kjartansson model of thermoelastic attenuation, Journal of Thermal Stresses, DOI: 10.1080/01495739.2023.2173685

To link to this article: https://doi.org/10.1080/01495739.2023.2173685

Published online: 08 Feb 2023.

Submit your article to this journal

View related articles

View Crossmark data

Full Terms & Conditions of access and use can be found at
https://www.tandfonline.com/action/journalInformation?journalCode=uths20

JOURNAL OF THERMAL STRESSES
https://doi.org/10.1080/01495739.2023.2173685

Taylor & Francis
Taylor & Francis Group

Check for updates

On Kjartansson model of thermoelastic attenuation

José M. Carcione[a,b], Faisal Alonaizi[c], Ayman N. Qadrouh[c], Mamdoh Alajmi[c], and Jing Ba[a]

[a]School of Earth Sciences and Engineering, Hohai University, Nanjing, China; [b]National Institute of Oceanography and Applied Geophysics, Trieste, Italy; [c]KACST, King Abdulaziz City for Science and Technology, Riyadh, Saudi Arabia

ABSTRACT

There is a mathematical analogy between the poroelastic and thermoelastic behavior of the compressional P wave, whose dissipation is due to the coupling between the elastic deformation and the phenomenon of pressure and heat diffusion, represented by Darcy's law and heat conduction, respectively. This attenuation effect is more pronounced in heterogeneous media, where conversion of the fast P wave to the slow (Biot) and thermal diffusive modes occurs at material interfaces. Specifically, the problem is to obtain the P-wave properties of a porous medium due to temperature gradients between the solid and fluid phases. Then, we consider a simplified one-dimensional porous medium and obtain the quality factor, Q, and phase velocity as a a function of frequency, based on an isostress condition and using Gassmann equation and the Kramers Kronig relations.The model allows for the incorporation of a relaxation time to simulate a proper wave-like behavior at high frequencies, avoiding in this way infinite velocities. Moreover, we perform a complete analysis varying the different parameters, namely, the heat conduction, the specific heat, the thermal expansion, the types of solid and fluid and the pore size.

ARTICLE HISTORY
Received 9 April 2021
Accepted 28 December 2022

KEYWORDS
Attenuation; porous media; thermoelasticity; velocity dispersion

1. Introduction

Thermoelasticity generalizes the classical theory elasticity, which deals with the interaction between deformation and temperature. In particular, the study of wave propagation considering the temperature field is relevant in several disciplines such as high-pressure high-temperature deep reservoirs in seismic exploration [1–3], geothermal studies [4] and seismology [5].

Although the work of Einar Kjartansson on seismic attenuation is mainly known because of his seminal article on the constant-Q model [6], he introduced in his PhD thesis an interesting and simple model of thermoelastic attenuation for a 1D poroelastic medium that can give physical insight into the effect of thermoelasticity on wave propagation [7]. To our knowledge, this model has not been published as a peer-review article.

Thermoelasticity couples the fields of deformation and temperature. An elastic source gives rise to a temperature field and wave attenuation, whereas a heat source induces anelastic deformations. This theory is useful in a variety of applications such as seismic attenuation in rocks and material science [1]. Zimmerman (2000) [8] stated that "the thermoelastic coupling parameter is usually very small, so that, although the temperature field influences the stresses and strains, the stresses and strains do not appreciably influence the temperature field". This means that elastic sources produce temperature fields that could hardly be detected, but as shown here,

CONTACT Jing Ba jba@hhu.edu.cn School of Earth Sciences and Engineering, Hohai University, Nanjing, China
© 2023 Taylor & Francis Group, LLC

the thermal effects have an influence on the properties of the P wave. Biot (1956) [9] derived the classical parabolic-type differential equations for the Fourier law of heat conduction. However, this theory has unphysical solutions, such as discontinuities and infinite velocities. Lord and Shulman (1967) [10] formulated a more physical system of equations by introducing the Maxwell-Vernotte-Cattaneo (MVC) relaxation time into the heat equation [11–13]. This theory leads to an attenuation kernel in analogy with the Maxwell model of viscoelasticity and predicts a physical wave-like behavior of the P wave [14,15].

The theory predicts two P waves and an S wave. The two P waves are an elastic wave and a thermal (T) wave having similar characteristics to the fast and slow P waves of poroelasticity. Rudgers (1990) [14] studied the propagation speeds and absorption coefficients of these waves as a function of frequency and [16] generalized the equations to the poroelastic case and developed a numerical algorithm for simulation of wave propagation based on the Lord-Shulman theory.

The T wave presents a diffusive behavior under certain conditions depending on viscosity, frequency and the thermoelastic constants. Generally, it is diffusive at low frequencies. Zener (1938) [1] explained the physics of thermoelastic attenuation in homogeneous media: "Stress inhomogeneities in a vibrating body give rise to fluctuations in temperature, and hence to local heat currents. These heat currents increase the entropy of the vibrating solid, and hence are a source of internal friction." Basically, the temperature variation caused by the passage of the P wave provides the gradient from which the thermal dissipation and attenuation occur.

P-wave dissipation has mainly been described first by phenomenological models represented by mechanical models made of springs and dashpots, as the standard-linear-solid system, also called Zener model. However Zener (1938) [1], obtained this model from thermoelasticity for thin rods as an approximation and the model was already known as a combination of a spring and the Kelvin-Voigt model. Similarly, the Biot relaxation peak in poroelasticity can also be approximated by the standard-linear solid [17,18]. Zener work already contains the concept of mode conversion (P wave to thermal mode), e.g., he explains P-wave dissipation due to the presence of "microscopic stress inhomogeneities arise from imperfections, such as cavities, and from the elastic anisotropy of the individual crystallites", in the same way as [19] explained attenuation in porous media due to mesoscopic-scale inhomogeneities (as P wave converted to Biot slow mode) (e.g Carcione (2014) [20],, Section 7.4).

To our knowledge, there is no composite theory for fluid-saturated porous media to describe the attenuation and phase velocity of P waves as a function of frequency in thermoelasticity, where all the properties can vary arbitrarily. Savage (1966) [21] considered a solid with empty voids (no fluid) and [2] a set of thin solid layers, and not all the thermoelasticity properties, since their theories were restricted to particular cases. For instance, in Armstrong's theory, only the Grüneisen ratio vary, which is a combination of the specific heat and thermal expansion [22]. The theory of thermo-poroelasticity, as Biot's poroelastic one, cannot describe realistic levels of attenuation in the homogeneous case, since the boundary conditions between the solid and fluid phases are not explicitly considered and the displacement field is that of a macroscopic volume, where the microscopic fields are averaged [9].

Realistic values of Q can be obtained with the present theory and those of Savage and Armstrong, where the heat flow (through the boundary conditions between the solid and fluid) is included. Kjartansson's original theory only predicts Q. Here, we modify and extend it to obtain the quality factor and wave (phase) velocity, implementing the more general Lord-Shulman heat equation, which includes a relaxation term. Moreover, we correct a mistake in his equation and compute the phase velocity using the Gassmann equation and the Kramers Kronig relations. Then, we perform a complete analysis varying the various thermoelasticity parameters, compare results to the mechanical model given by the standard-linear solid or Zener and develop an alternative theory given by the isostrain condition, since Kjartansson's theory is an isostress one. The present theory is analogous to the wave-induced fluid flow attenuation observed at the

mesoscopic scale in heterogeneous porous media , such as those described by the Biot theory [19]. The difference is that in the present theory it is heat to flow instead of a fluid.

2. Thermoelasticity equations

Following [7], let us consider an idealized 1D medium porous medium with a flat pore (Figure 1), whose constitutive equation relates the stress σ, the strain ϵ and the temperature T above a reference absolute temperature T_0 for the state of zero stress and strain. A random set of uncorrelated pores should have a similar behavior as a single pore. In a linear 1D isotropic medium, the equation of momentum conservation and stress-strain relations of thermoelasticity describing P waves are [[9], Eq. (2.2)); [15]]

$$\sigma_{,x} = \rho\ddot{u}, \quad \text{and} \quad \sigma = K_I\epsilon - \beta T \tag{1}$$

where u is the displacement, $\epsilon = u_{,x}$ is the strain, K_I is the isothermal P-wave modulus, β is the thermal expansion, ρ is the mass density and "$_{,x}$" denotes the spatial derivative. This quantity is usually expressed as $\beta = 3\alpha K_I$, where α is the coefficient of linear thermal expansion (the volumetric one is 3α).

On the other hand, the law of generalized heat equation, or strain-temperature field equation, is [15]

$$\gamma T_{,xx} = c(\dot{T} + \tau\ddot{T}) + \beta T_0(\dot{\epsilon} + \tau\ddot{\epsilon}), \tag{2}$$

where γ is the coefficient of heat conduction (or thermal conductivity), c is the volumetric specific heat, "$_{,xx}$" denotes the second spatial derivative, and a dot above a variable denotes time derivative. This equation is a generalization of Eq. (32.2) in [23] and Eq. (4) in [22], by introducing a MVC relaxation time τ to avoid unphysical infinite velocities of the P wave at high frequencies [10]. In ([24], Eq. 1.2.15), equation (2), with $\tau = 0$, is called displacement-temperature field equation. Equation (2) is based on the theory of Lord-Shulman, where the two (thermal and strain-rate) relaxation times are the same. In ([25], Eq. 5), we have also considered the theory of [26], where these relaxation times differ. Clearly, the second theory may provide better fits to real data, due to the additional parameters.

Appendix A and Figure 2 illustrate the physics, showing that there are two waves, i.e, the P wave and the thermal or T wave, which is diffusive at low frequencies. The dashed lines correspond to the classical theory of thermoelasticity with $\tau = 0$. As can be seen, the P-wave velocity is infinite and there are unphysical discontinuities, and it can be shown that the inverse quality factor tends to infinite at high frequencies, while it is a relaxation peak for $\tau \neq 0$.

The correspondence between the properties in Eqs. (5.2) and (5.3) in [7] and those of equations (1) and (2) given here [$\tau = 0$ in [7]] are $D \equiv 1/(1/D - \beta\zeta/\gamma)$ (see below), $K \equiv K_I$, $b \equiv -b$

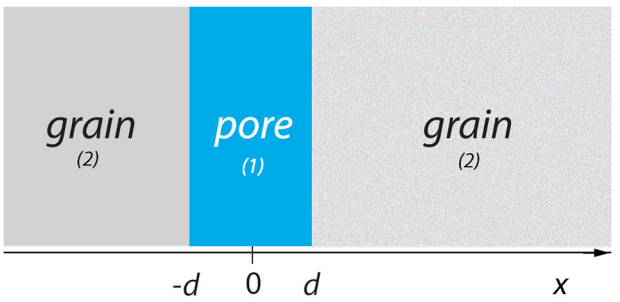

Figure 1. 1D porous medium. The numbers refer to the subindices related to the properties in the main text.

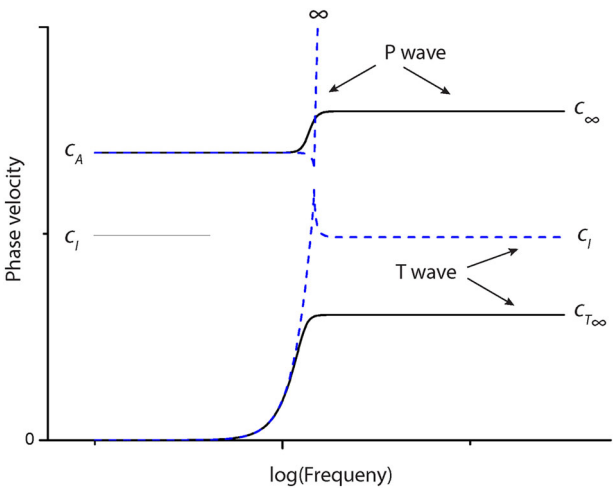

Figure 2. Phase velocities as a function of frequency, showing the low- and high-frequency velocities. The dashed blue lines correspond to $\tau = 0$ (the classical theory of thermoelasticity). c_A and c_I indicate the adiabatic and isothermal velocities. This is the case $c_A > \sqrt{2}c_I$ in ([14], Figure 2), where it is the P wave to have the singularity. For $c_A < \sqrt{2}c_I$, the T wave has infinite velocity and the P wave approaches the isothermal velocity at high frequencies.

(see below) and $\alpha K \equiv 3\alpha K_I$. Equation (2) holds for locally constant properties, while at interfaces, continuity of temperature and heat flow must be satisfied.

Combining equations (1) and (2), we obtain

$$\gamma T_{,xx} = \zeta\left(\frac{\dot{T} + \tau\ddot{T}}{b} + \dot{\sigma}\right), b = \frac{\zeta}{c + \beta\zeta}, \zeta = \frac{\beta T_0}{K_I}. \tag{3}$$

Let us consider a time dependence $\exp(\mathrm{i}\omega t)$, where ω is the real angular frequency and t is time.

Equation (3) becomes

$$\mathrm{i}\omega(1 + \mathrm{i}\omega\tau)\hat{T} = D\hat{T}_{,xx} - \mathrm{i}\omega b, \hat{T} = \frac{T}{\sigma}, D = \frac{b\gamma}{\zeta} = \frac{\gamma}{c + \beta^2 T_0/K_I}, \tag{4}$$

and we have assumed that σ is spatially constant for a flat pore (isostress condition).

The characteristic equation of the homogeneous part of equation (4), for a general solution of the form $\exp(\xi x)$, gives the roots

$$\xi = \pm\sqrt{\frac{\mathrm{i}\omega(1 + \mathrm{i}\omega\tau)}{D}}. \tag{5}$$

For $\tau = 0$, equation (5) becomes

$$\xi d = \pm\sqrt{\mathrm{i}\omega\eta}, \eta = \frac{d^2}{D}, \tag{6}$$

where η is the relaxation time defined by [7].

It is shown in Appendix B that the solution of equation (4), with proper boundary conditions at the solid-fluid interface, is

$$\hat{T} = \begin{cases} A_1\cosh(\xi_1 x) - b_1, & |x| \le d, \\ A_2\exp(-\xi_2|x|) - b_2, & |x| > d, \end{cases} \tag{7}$$

where

$$A_1 = \frac{b_1 - b_2}{\cosh(\xi_1 d) + r\sinh(\xi_1 d)}, \quad r = \frac{\gamma_1}{\gamma_2}\sqrt{\frac{D_2}{D_1}} \tag{8}$$

and

$$A_2 = -\frac{r\sinh(\xi_1 d)}{\exp(-\xi_2 d)} \cdot A_1. \tag{9}$$

Equation (7) is a generalization of Eqs. (5.12) and (5.13) of [7], but note that there is a typo (or a mistake) in coefficient A_1 in ([7], Eq. 5.16): factor $\sinh(\xi_2 d)$ in the denominator should be $\sinh(\xi_1 d)$.

Based on equation (7), the heat-diffusion length L is obtained by setting $|\xi x| = |\xi L| = 1$. It is $\tau = 0$, this gives

$$L = \sqrt{\frac{D}{\omega}}. \tag{10}$$

The temperature will be equilibrated if L is comparable or smaller than the pore size. For small diffusion lengths (e.g. high frequencies) the temperature will not be equilibrated and this is the cause of attenuation and velocity dispersion. The relaxation frequency, f_R, is approximately obtained if the diffusion length L is of the order of the pore size d, i.e., if [from (10)],

$$f_R \approx \frac{D}{8\pi d^2}. \tag{11}$$

The skin depth, L', also quantifies the diffusion length. By definition, $\exp[-\mathrm{Im}(\xi)L'] = \exp(-1)$, which gives $L' = L/\sqrt{2}$.

The complex compliance (inverse of stiffness M) can be obtained from equation (1) as

$$S(\omega) = \frac{1}{M(\omega)} = \frac{1}{K_I}\left[1 + \beta\hat{T}(\omega)\right]. \tag{12}$$

Let us introduce the porosity ϕ. Then, the size of the grain is

$$X = 2d\left(\frac{1}{\phi} - 1\right) = \frac{2d}{\epsilon}, \quad \epsilon = \frac{\phi}{1-\phi}, \tag{13}$$

where ϵ is the so-called void ratio (e.g., if $\phi = 0.2$, $\epsilon = 0.25$, $X = 8\ d$). Integrating equation (12) over the pore and one grain gives the average compliance

$$\bar{S} = \frac{1}{2d + X}\int_{-d}^{d+X} S dx = \frac{\phi}{2d}\left(\int_{d}^{d+X} S_2 dx + \int_{-d}^{d} S_1 dx\right). \tag{14}$$

After some calculations and replacing A_1 and A_2, we obtain

$$\bar{S} = \frac{1}{\bar{K}} + \bar{b} + \frac{\phi(b_1 - b_2)}{d[r + \coth(\xi_1 d)]}\left(\frac{\beta_1}{\xi_1 K_{I1}} + \frac{\beta_2}{2\xi_2 K_{I_2}} \cdot r[\exp(-\xi_2 X) - 1]\right), \tag{15}$$

where

$$\frac{1}{\bar{K}} = \frac{\phi}{K_{I1}} + \frac{1-\phi}{K_{I2}}, \quad \bar{b} = \phi\frac{b_1\beta_1}{K_{I1}} + (1-\phi)\frac{b_2\beta_2}{K_{I2}}. \tag{16}$$

Then, the quality factor is given by [20]

$$Q = -\frac{\mathrm{Re}(\bar{S})}{\mathrm{Im}(\bar{S})}. \tag{17}$$

Table 1. Kjartansson (1980) [7] thermal properties of rocks and fluids.

Rock	T_0 °K	p MPa	ρ [·]	α 10^{-6} [·]	K_I [·]	c [·]	γ [·]	$\delta = \frac{K_A - K_I}{K_I} \times 10^{-4}$	D' 10^{-6} [·]
limestone	300	300	2710	1.13	76	2.28	3.85	1.15	1.7
quartzite	300	300	2640	0.37	42	1.98	8.16	0.078	4.1
granite	300	100	2650	2.6	46	1.56	–	5.38	–
water	293	0.1	990	67	2.2	4.15	0.6	62.8	0.14
water	554	10	773	733	0.55	3.89	0.59	3788	0.15
steam	373	0.1	0.6	967	10^{-4}	0.001218	0.024	2577	20
nitrogen	300	0.1	1.2	1110	10^{-4}	0.00086	0.026	3868	30

Table 2. Thermal properties of rocks and fluids.

Rock	T_0 °K	ρ [·]	β MPa/° K	K_I [·]	c [·]	γ [·]	D 10^{-6} [·]	ζ	b °K/Pa
limestone	300	2710	0.258	76	2.28	3.85	1.7	0.001	$4.46 \cdot 10^{-10}$
quartzite	300	2640	0.047	42	1.98	8.16	4.1	0.00033	$1.7 \cdot 10^{-10}$
granite	300	2650	0.36	46	1.56	–	–	0.0023	$1.5 \cdot 10^{-9}$
water	293	990	0.442	2.2	4.15	0.6	0.14	0.059	$1.4 \cdot 10^{-8}$
water	554	773	1.21	0.55	3.89	0.59	0.11	1.22	$2.27 \cdot 10^{-7}$
steam	373	0.6	0.00029	10^{-4}	0.001218	0.024	15.5	1.08	$7.06 \cdot 10^{-4}$
nitrogen	300	1.2	0.00033	10^{-4}	0.00086	0.026	21.7	1	$8.38 \cdot 10^{-4}$

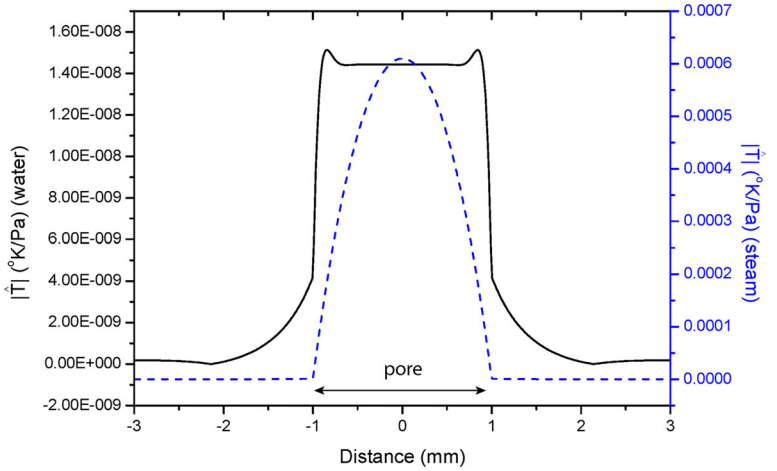

Figure 3. Absolute value of $\hat{T}$ as a function of distance at $f = 10$ Hz. The solid-black and dashed-blue lines correspond to water and steam as pore-filling material, respectively.

The isostress condition yields a Reuss modulus $\bar{K}$ (harmonic average) to describe the stiffness of the medium, i.e., related to a suspension of particles in a fluid, with a frame modulus equal to zero. This condition is a good approximation to obtain the thermoelastic loss, since the heat flux is not affected as the stiffness and wave velocity by the effect of the grain contacts, which mainly determine the frame properties. A specific approach to obtain the low-frequency velocity is the Gassmann theory [20, 27], which includes the frame modulus. The Gassmann wet-rock modulus is

$$\bar{K}_I = \frac{K_{I2} - K_m + \phi K_m (K_{I2}/K_{I1} - 1)}{1 - \phi - K_m/K_{I2} + \phi K_{I2}/K_{I1}}, \tag{18}$$

where K_m is the dry-rock modulus and index "I" indicates isothermal. In particular, $\bar{K}_I = \bar{K}$ for $K_m = 0$. We use the Krief equation [28],

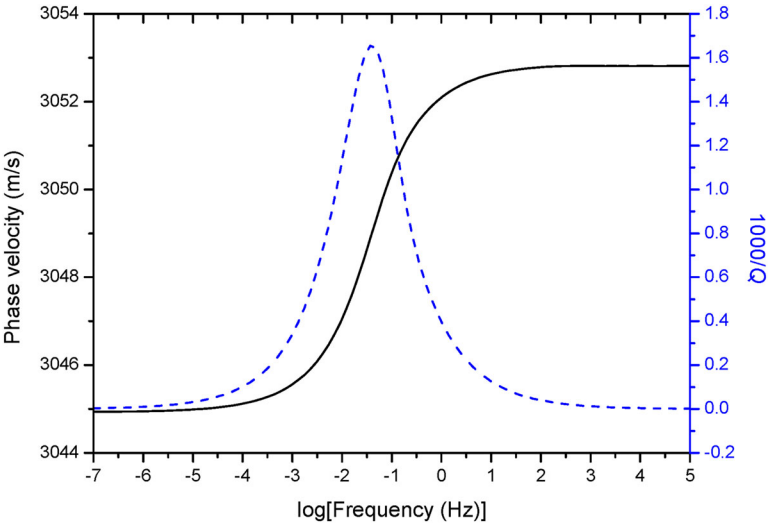

Figure 4. Phase velocity (solid line) and quality factor (dashed line) of a porous medium saturated with water.

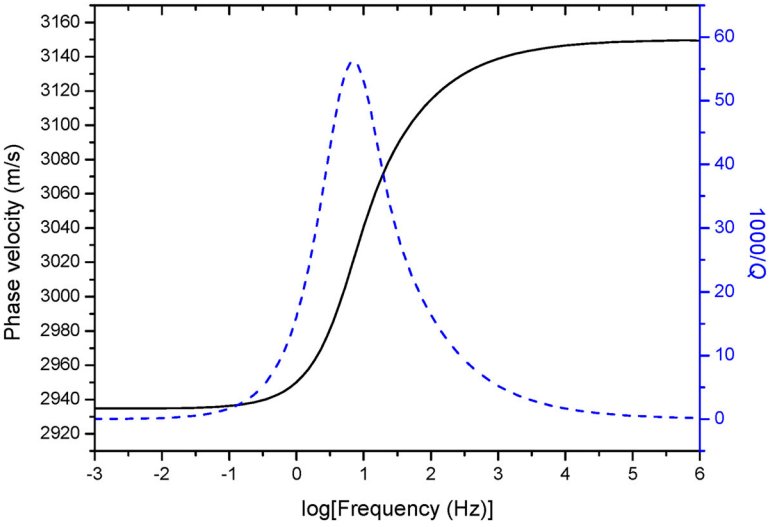

Figure 5. Phase velocity (solid line) and quality factor (dashed line) of a porous medium saturated with steam.

$$K_m = K_{I2}(1-\phi)^{A/(1-\phi)}, \tag{19}$$

where A is a dimensionless parameter (a value $A = 3$ is assumed here).

As shown in Appendix A for a single-phase medium, the zero-frequency velocity is the adiabatic velocity c_A, not the isothermal velocity (Figure 2). From equations (A.3) and (A.4), we have

$$\bar{c}_A = \sqrt{\bar{c}_I^2 + \frac{\bar{\beta}^2 T_0}{\bar{\rho}\bar{c}}}, \tag{20}$$

where

$$\bar{c}_I = \sqrt{\frac{\bar{K}_I}{\bar{\rho}}}, \tag{21}$$

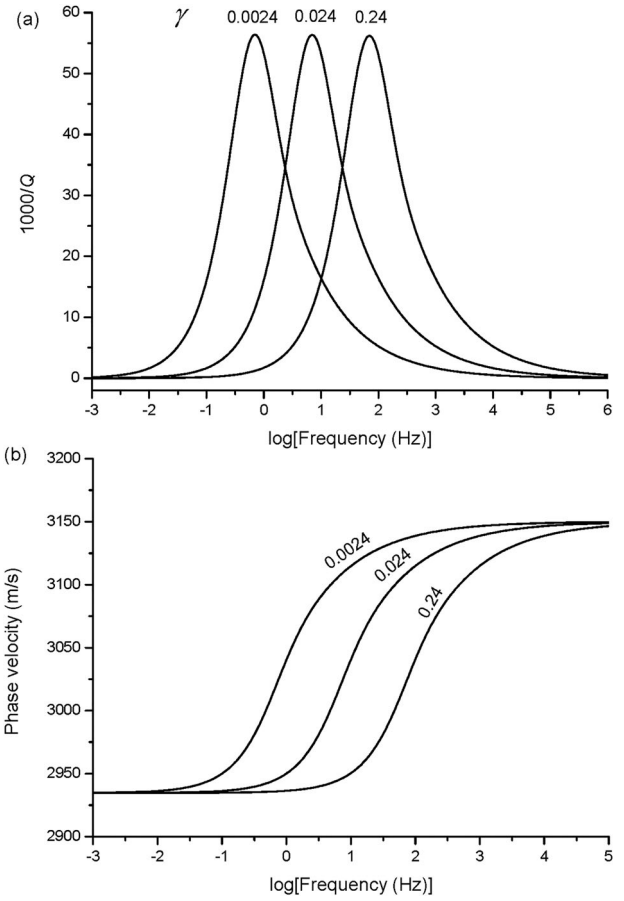

Figure 6. Quality factor (a) and phase velocity (b) as a function of frequency for a porous medium saturated with steam, for different values of γ given in m kg/(s^3 $^\circ$ K).

the Gassmann velocity,

$$\bar{\rho} = \phi\rho_1 + (1-\phi)\rho_2. \tag{22}$$

and we assume

$$\bar{\beta} = \phi\beta_1 + (1-\phi)\beta_2, \quad \bar{c} = \phi c_1 + (1-\phi)c_2. \tag{23}$$

To obtain the phase velocity c_p versus frequency, we use an approximation reported by [29], based on the Kramers-Kronig relations [22, 30],

$$\frac{c_A}{c_p(\omega)} = 1 - \frac{1}{\pi}\int_{\omega_0}^{\omega} \frac{Q^{-1}(\omega')}{\omega'}\, d\omega', \tag{24}$$

where ω_0 is very close to zero.

We can obtain the complex wave modulus, M, associated to this phase velocity and Q factor. It is shown in [22] that

$$M(\omega) \approx \bar{\rho}\, c_p^2(\omega)\left(1 + \frac{\mathrm{i}}{Q(\omega)}\right). \tag{25}$$

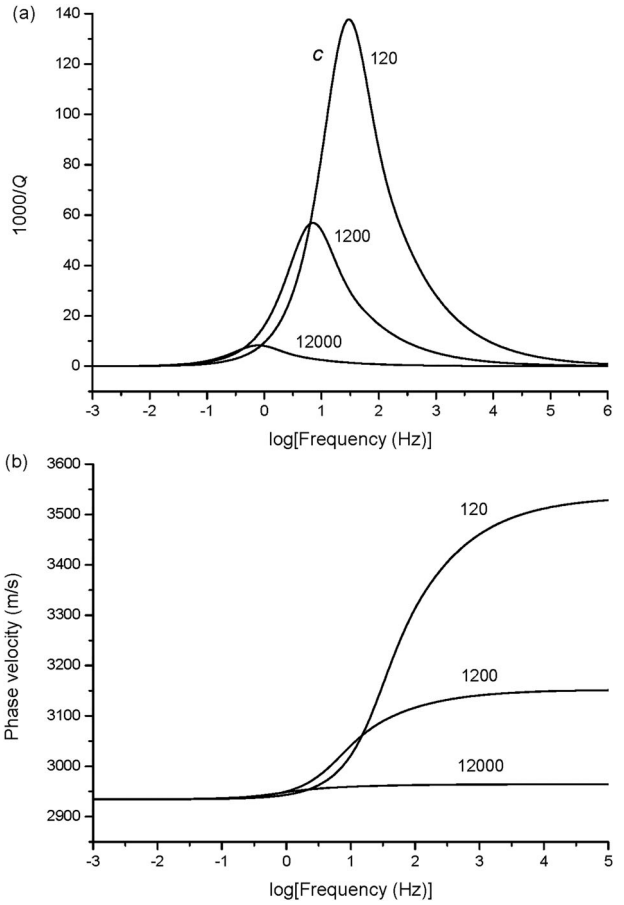

Figure 7. Quality factor (a) and phase velocity (b) as a function of frequency for a porous medium saturated with steam, for different values of c given in kg/(m $s^{2\circ}$ K).

Another approach other than the isostress condition to obtain the quality factor from the complex modulus is to use the isostrain condition (for completeness it is given in Appendix C). However, the contribution to the thermoelastic loss is minimal compared to the first case. It is well known that in a composite material, the stiffness lies between the low-frequency limit given by the Backus averaging ([20], Eq. 333) and the high-frequency-limit given by the time-average equation ([20], Eqs. 1.188(2) and 8.415, respectively). If M_1 and M_2 are the moduli of two phases of proportion ϕ and $1-\phi$, the respective moduli are

$$\left(\frac{\phi}{M_1}+\frac{1-\phi}{M_2}\right)^{-1} \quad \text{and} \quad \left(\frac{\phi}{\sqrt{M_1}}+\frac{1-\phi}{\sqrt{M_2}}\right)^{-1}.$$

The former is compatible with the isostress condition (harmonic average of the single stiffnesses), while at high frequencies the second implies the harmonic average of the square root of the stiffnesses, and the solution, if the first phase a fluid, is closer to the first one than to the isostrain modulus $\phi M_1 + (1-\phi)M_2$.

3. Examples

Typical acoustic and thermoelastic properties of rocks are given in Tables 1 and 2, taken from [7] (see Appendix D). First, we choose quartzite as the solid material and water and steam as fluids

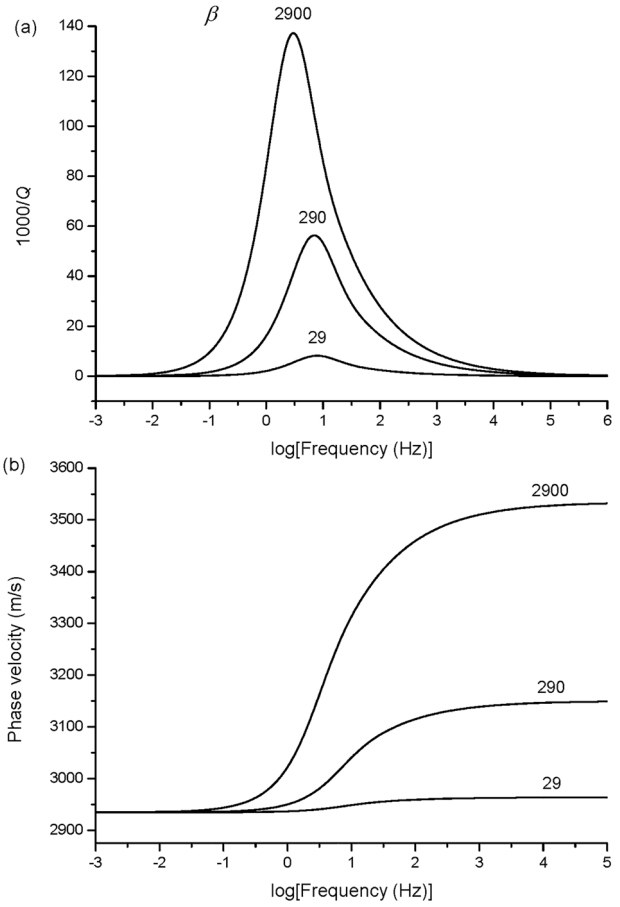

Figure 8. Quality factor (a) and phase velocity (b) as a function of frequency for a porous medium saturated with steam, for different values of β given in kg/(m s$^{2\,\circ}$ K).

at 0.1 MPa, with $T_0 = 300\,^\circ$ K. Figure 3 shows the normalized field $\hat{T}$ as a function of distance, where it is clear that the thermoelastic effect of steam is several orders of magnitude higher than that of water.

Figures 4 and 5 show the phase velocity and dissipation factors as a function of frequency. The attenuation and velocity dispersion are much stronger in the porous medium saturated with steam, with a minimum Q factor at the peak of approximately 18 and heat flows mainly in the fluid due to its favorable thermal properties. In the case of water as pore fluid, the quality factor at the peak is 590 and is located at much lower frequencies. Similar peaks have been obtained by [21] and [2] for empty voids and layers, respectively.

Now, let us consider variations of the thermal properties of steam around the reference values of Table 2. Figures 6–8 show the quality factor and phase velocity for different values of γ_1, c_1 and β_1, respectively. Increasing the thermal conductivity implies a shift of the relaxation peak to the high frequencies, keeping the maximum value constant (Figure 6). This does not mean that attenuation is the same. For instance, a plane wave $\exp[\mathrm{i}(\omega t - \kappa x)]\exp(-Ax)$ that has traveled a distance x, where κ is the real wavenumber, has the attenuation factor

$$A = \frac{\pi\omega}{2\pi Q c_p} \propto \omega,$$

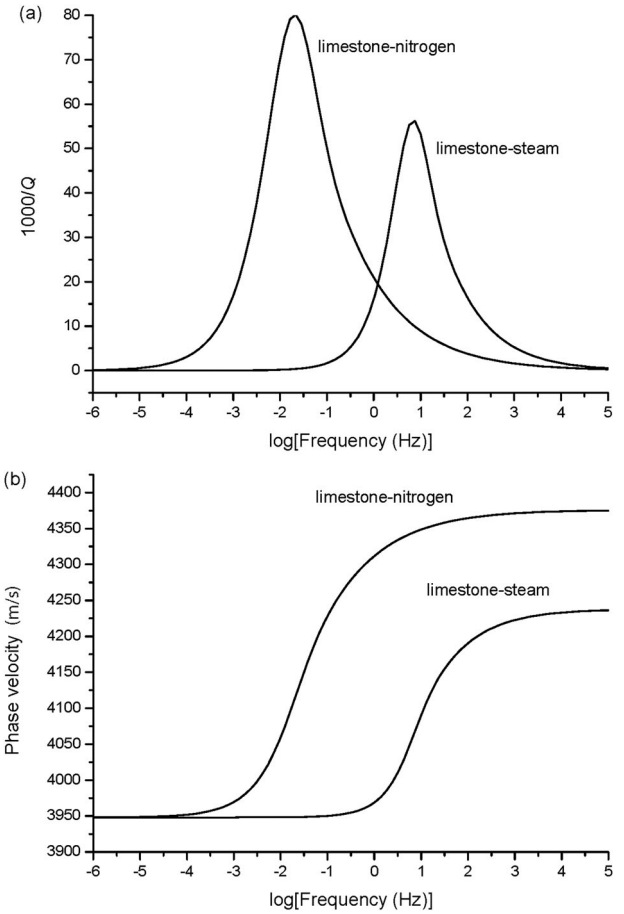

Figure 9. Quality factor (a) and phase velocity (b) as a function of frequency for a porous medium saturated with steam and nitrogen. The solid is limestone.

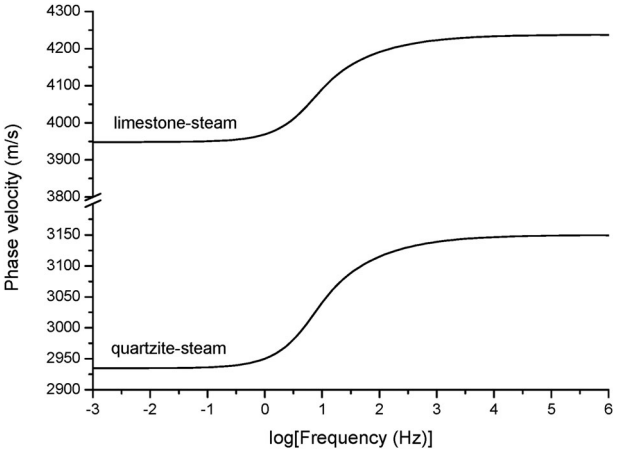

Figure 10. Phase velocity as a function of frequency for a porous medium saturated with steam. The solid is quartzite or limestone. The quality factor (not shown) is similar to that of Figure 5.

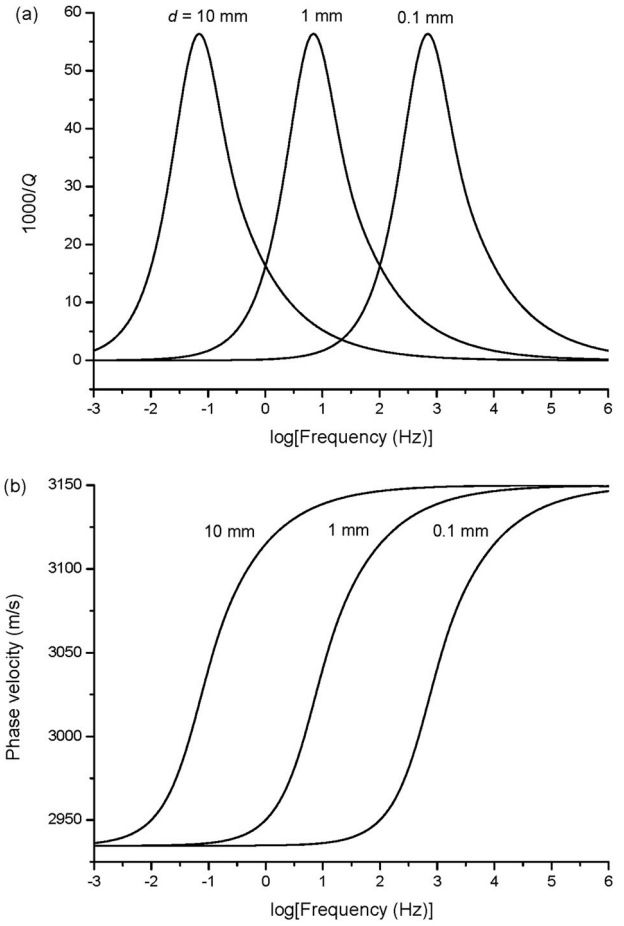

Figure 11. Quality factor (a) and phase velocity (b) as a function of frequency for a porous medium saturated with steam. The solid is quartzite and three values of the pore size, d, are considered.

([20], Eq. 2.123), since the product Qc_p is not significantly affected. We can see that the higher the frequency, the higher the damping the wave suffers for the same travel distance. On the other hand, decreasing c_1 or increasing β_1 implies more attenuation, moving the peak to the low frequencies in both cases (Figures 7 and 8).

The effect of the type of fluid with the same frame is shown in Figure 9, where the solid is limestone and the fluids are steam and nitrogen. In the latter case, the peak is located at lower frequencies. The effect of the type of solid is only significant in the phase velocity (Figure 10), with higher velocities in the case of limestone, since it is a stiffer material.

Then, we consider three values of the pore size $2d$. Figure 11 shows the quality factor (a) and phase velocity (b) as a function of frequency for a medium composed of quartzite and steam. The effect of varying d is to move the relaxation peak to the high frequencies, when d decreases, in agreement with equation (11). A quite precise value of the peak frequency for this particular model is

$$f_{\text{peak}} \approx \frac{5D_1}{4\pi d^2},$$

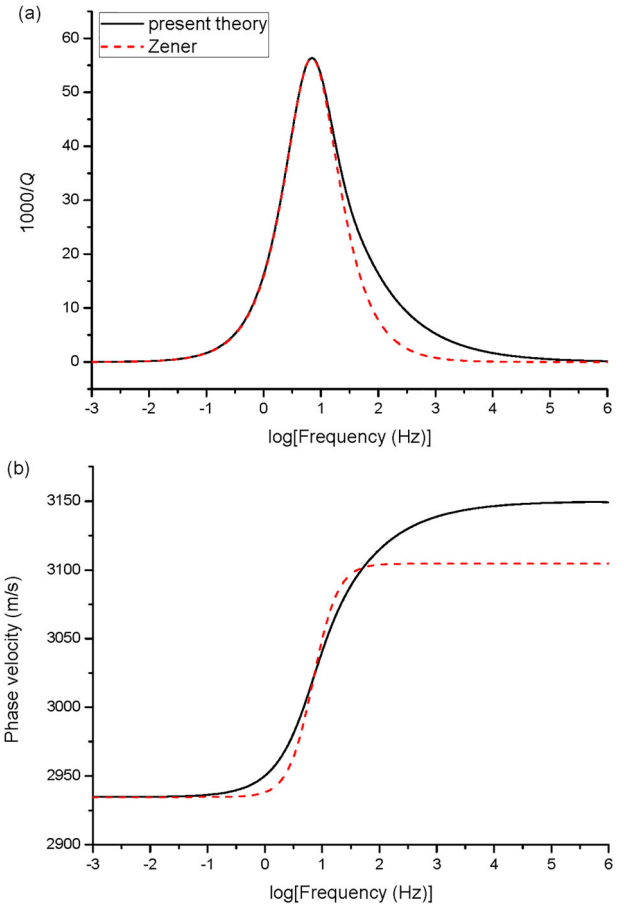

Figure 12. Quality factor (a) and phase velocity (b) as a function of frequency for a porous medium saturated with steam. Comparison between the present theory and the Zener (standard-linear-solid) model. The properties correspond to Figure 5.

which is analogous to Eq. 7.449 in [20], regarding the location of the wave-induced fluid-flow (mesoscopic) peak in poroelasticity.

Transient wavefields are effectively computed in the space-time domain, where the Zener model (see Appendix E) is usually used to describe the velocity dispersion and attenuation [31]. Figure 12 compares the dissipation factor (a) and phase velocity (b) of the Zener (or standard-linear-solid) model with those of the present theory, corresponding to the case of Figure 5. i.e., a porous medium saturated with steam, where $f_0 = 7\,\text{Hz}$, the minimum quality factor is $Q_0 = 17.75$ and $Z_0 = \bar{\rho} c_A^2$. The fit has been achieved by assuming the same low-frequency velocity. As can be seen, the agreement is acceptable in the seismic band (from 5 to 100 Hz), indicating that the Zener model can be a good approximation for numerical simulations. A better approximation can be achieved with the Cole-Cole model, but its implementation in numerical modeling requires the computation with fractional time derivatives [32].

The strain-displacement equation (2) used here is the classical one introduced by [10]. We consider the formulation with a complex wavenumber and a real temporal frequency, because we are interested in traveling waves [see Section 2.3 in [20]]. An alternative formulation is to consider a complex frequency and a real wavenumber to describe stationary waves [Section 2.3.1 in [20]]. Traveling waves are of main interest in seismology and electromagnetic geophysical methods, and usually the differential equations governing the field propagation are based on a source and initial conditions [33].

4. Conclusions

We present a simple, though general, model of thermoelastic attenuation in porous media. The loss mechanism is that of conversion of mechanical energy in the form of deformations and/or waves to the slow thermal mode, similar to wave-induced fluid-flow attenuation in poroelasticity. The model provides the quality factor as a function of frequency and the phase velocity, based on the Kramers-Kronig relations and can be used to obtain physical insight to analyze the effect of the elastic and thermoelastic properties. The dissipation factor (reciprocal of Q) resemble peaks obtained with the standard-linear-solid (Zener) mechanical model, although there are some differences, mainly at high frequencies. Strictly, the Lord-Shulman theory is used, although the relaxation peaks are located at low frequencies, where the thermal mode is diffusive.

The type of pore infill is highly dominant, since gases imply a higher contrast with the grain properties. It is clear that the thermoelastic effect of steam on the spatial temperature profile is several orders of magnitude higher than that of water and that attenuation and velocity dispersion are much stronger. Similar peaks have been obtained in the past for empty voids and layering.

We found that increasing the thermal conductivity of the fluid implies a shift of the relaxation peak to the high frequencies, keeping the maximum value of Q constant, although the higher the frequency, more damping the wave suffers for the same travel distance. Moreover, decreasing the specific heat or increasing the thermal expansion implies more attenuation, moving the peak to the low frequencies in both cases.

The effect of the type of fluid (same skeleton) is to shift the location of the relaxation peak and maximum attenuation, whereas the effect of the solid is only significant in the phase velocity, with higher velocities in the case of a stiffer grain material, as expected. The relaxation peak moves to the high frequencies when the pore size decreases, in agreement with the mesoscopic-loss behavior in poroelasticity.

Numerical simulations can be achieved in the space-time domain by using the Zener model as an approximation of the relaxation peak and velocity dispersion, but the the Zener parameters have to be calibrated with the theory. The model can be extended to 2D and 3D space, in particular, the first step will be to consider a set of thin layers (compared to the wavelength) of infinite lateral extent, as the White mesoscopic-loss model.

Appendix A. Dispersion equation. Classical and Lord-Shulman theories

The difference between the classical theory of thermoelasticity [9] and that of [10] is the introduction of a relaxation time τ in the heat equation that transform this equation from parabolic to hyperbolic in the mathematical terminology (e.g., ([34], Chapter 4), i.e., from diffusive-like to wave-like. The idea dates back to James Clerk Maxwell when he dealt with wave propagation in gases [11]. This avoids unphysical velocities of the P wave. To show this, let us consider a space-time dependence $\exp(\mathrm{i}\omega t - \mathrm{i}kx)$, where ω is the real angular frequency,

$$k = \frac{\omega}{v}, \tag{A.1}$$

is the complex wavenumber, v is the complex velocity and t is the time.

If the elasticity and heat equations (1) and (2) are uncoupled, the velocity of the P wave is simply $v = \sqrt{K_I/\rho}$, but if these equations are coupled, the P-wave velocity is affected as follows. Equations (1) and (2) give the following dispersion relation [15, 32]

$$v^4 - (c_A^2 + M)v^2 + Mc_I^2 = 0, \quad M = \frac{\mathrm{i}\omega a^2}{1 + \mathrm{i}\omega\tau}, \tag{A.2}$$

where

$$c_I = \sqrt{\frac{K_I}{\rho}} \quad \text{and} \quad c_A = \sqrt{c_I^2 + c_T^2} \tag{A.3}$$

are the isothermal and adiabatic velocities, respectively,

$$c_T = c_I\sqrt{\frac{\zeta\beta}{c}}, \quad a = \sqrt{\frac{\gamma}{c}}, \quad \zeta = \frac{\beta T_0}{K_I}. \tag{A.4}$$

Equation (A.2) has the solutions:

$$2v^2 = c_A^2 + M \pm \sqrt{(c_A^2 + M)^2 - 4Mc_I^2}. \tag{A.5}$$

There are two P-wave solutions, an elastic P wave (plus sign) and a thermal T wave (minus sign). At $\omega = 0$ we have two real solutions: $v = 0$ (T wave) and $v = c_A$ (P wave). At infinite frequency, it is $v = \infty$ (P wave) and $v = c_I$ (T wave).

[14] considers

$$\tau = \frac{a^2}{c_I^2} \tag{A.6}$$

for his lattice model [see his eqs. (34), (37) and (58)]. For $\omega \to \infty$, we have $M \to a^2/\tau = c_I^2$ and the solution is

$$2v^2 = c_A^2 + c_I^2 \pm \sqrt{(c_A^2 + c_I^2)^2 - 4c_I^4}, \tag{A.7}$$

where the plus and minus signs correspond to the P and T waves, respectively. Denoting the velocities by c_∞ and $c_{T\infty}$, respectively, we have $c_{T\infty} < c_I < c_A < c_\infty$. The relaxed and unrelaxed P-wave moduli of the model – with the choice (A.6) – are

$$K_A = \rho c_A^2 \quad \text{and} \quad K_\infty = \frac{\rho}{2}\left[c_A^2 + c_I^2 + \sqrt{(c_A^2 + c_I^2)^2 - 4c_I^4}\right], \tag{A.8}$$

respectively.

Appendix B. Isostress conditions

The solution for the system shown in Figure 1 must be bounded at $x = \pm\infty$. Then, a general solution must be

$$\begin{aligned} \hat{T} &= A_1 \exp(+\xi_2 x) - b_2, \quad x < -d, \\ \hat{T} &= A_2 \exp(\xi_1 x) + A_3 \exp(-\xi_1 x) - b_1, \quad |x| \le d, \\ \hat{T} &= A_4 \exp(-\xi_2 x) - b_2, \quad x > d, \end{aligned} \tag{B.1}$$

where the subindices 1 and 2 indicate the fluid and grain, respectively. To obtain A_1-A_4, we impose boundary conditions at $x = -d$ and $x = d$, i.e., continuity of temperature and thermal current

$$\hat{T}_1 = \hat{T}_2 \quad \text{and} \quad \gamma_1 T_{1,x} = \gamma_2 T_{2,x}, \tag{B.2}$$

respectively (e.g., ([24], Eq. 2.1.5). We obtain

$$\begin{aligned} &A_1 \exp(-\xi_2 d) - b_2 = A_2 \exp(-\xi_1 d) + A_3 \exp(\xi_1 d) - b_1, \\ &\xi_2\gamma_2 A_1 \exp(-\xi_2 d) = \xi_2\gamma_2 A_2 \exp(-\xi_1 d) - \xi_1\gamma_1 A_3 \exp(\xi_1 d), \\ &A_2 \exp(\xi_1 d) + A_3 \exp(-\xi_1 d) - b_1 = A_4 \exp(-\xi_2 d) - b_2, \\ &\xi_1\gamma_1 A_2 \exp(\xi_1 d) - \xi_1\gamma_1 A_3 \exp(-\xi_1 d) = -\xi_2\gamma_2 A_4 \exp(-\xi_2 d). \end{aligned} \tag{B.3}$$

Replacing A_1 and A_4 from the first and fourth equations into the second and third equations, respectively, we obtain

$$\begin{pmatrix} a_{11} & a_{12} \\ a_{21} & a_{22} \end{pmatrix} \cdot \begin{pmatrix} A_2 \\ A_3 \end{pmatrix} = \begin{pmatrix} q \\ -q \end{pmatrix}, \tag{B.4}$$

where

$$\begin{aligned} a_{11} &= +\exp(-\xi_1 d)(\xi_2\gamma_2 - \xi_1\gamma_1), \\ a_{12} &= +\exp(+\xi_1 d)(\xi_2\gamma_2 + \xi_1\gamma_1), \\ a_{21} &= -\exp(+\xi_1 d)(\xi_2\gamma_2 + \xi_1\gamma_1), \\ a_{22} &= -\exp(-\xi_1 d)(\xi_2\gamma_2 - \xi_1\gamma_1), \\ q &= -\xi_2\gamma_2(b_2 - b_1), \end{aligned} \tag{B.5}$$

Solving for A_2 and A_3 and calculating A_1 and A_4 from the first and fourth equations (B.3), we obtain the coefficients

$$A_1 = A_4 = \left[A_2 \exp(-\xi_1 d) + A_3 \exp(\xi_1 d) + b_2 - b_1\right] \exp(\xi_2 d),$$
$$A_2 = A_3 = \frac{q}{\det}(a_{22} + a_{12}), \tag{B.6}$$
$$\det = a_{11}a_{22} - a_{12}a_{21},$$

Appendix C. Isostrain conditions

The equivalent to equation (4) for isostrain conditions is

$$\mathrm{i}\omega(1 + \mathrm{i}\omega\tau)\check{T} = D'\check{T}_{,xx} - \mathrm{i}\omega b', \quad \check{T} = \frac{T}{\epsilon}, \quad D' = \frac{\gamma}{c}, \quad b' = \frac{(1 + \mathrm{i}\omega\tau)\beta T_0}{c} \tag{C.1}$$

and we have assumed that the strain ϵ is spatially constant. The roots have the same form of equation (5)

$$\xi' = \pm\sqrt{\frac{\mathrm{i}\omega(1 + \mathrm{i}\omega\tau)}{D'}}, \tag{C.2}$$

as well as the solution that of equation (7),

$$\hat{T} = \begin{cases} A_1' \cosh(\xi_1' x) - b_1', & |x| \le d, \\ A_2' \exp(-\xi_2'|x|) - b_2', & |x| > d, \end{cases} \tag{C.3}$$

where

$$A_1' = \frac{b_1' - b_2'}{\cosh(\xi_1' d) + r' \sinh(\xi_1' d)}, \quad r' = \frac{\gamma_1}{\gamma_2}\sqrt{\frac{D_2'}{D_1'}} \tag{C.4}$$

and

$$A_2' = -\frac{r' \sinh(\xi_1' d)}{\exp(-\xi_2' d)} \cdot A_1'. \tag{C.5}$$

The complex stiffness can be obtained from equation (1) as

$$M'(\omega) = K_I - \beta\check{T}(\omega). \tag{C.6}$$

Integrating equation (C.6) over pore and grain gives the average stiffness

$$\bar{M}' = \frac{1}{2d + X}\int_{-d}^{d+X} M' dx = \frac{\phi}{2d}\left(\int_{d}^{d+X} M_2' dx + \int_{-d}^{d} M_1' dx\right). \tag{C.7}$$

After some calculations and replacing A_1' and A_2', we obtain

$$\bar{M}' = \bar{K}' - \bar{b}' - \frac{\phi(b_1' - b_2')}{d\left[r' + \coth(\xi_1' d)\right]}\left(\frac{\beta_1}{\xi_1'} + \frac{\beta_2}{2\xi_2'} \cdot r'\left[\exp(-\xi_2' X) - 1\right]\right), \tag{C.8}$$

where

$$\bar{K}' = \phi K_{I1} + (1 - \phi)K_{I2}, \bar{b}' = \phi \quad b_1'\beta_1 + (1 - \phi)b_2'\beta_2 \tag{C.9}$$

are arithmetic (Voigt) averages.

Appendix D. Acoustic and thermal properties

These data is taken and modified from ([7], p. 67, Table 5.2), based on the notation of [15]. The units are given in the MKS system:

$$\begin{array}{l}\text{absolute temperature, } T_0: {}^{\circ}\text{K},\\ \text{pressure, } p: \text{MPa}: 10^6\ \text{kg}/(\text{m s}^2),\\ \text{density, } \rho: \ \text{kg}/\text{m}^3\\ \text{linear coefficient of thermal expansion, } \alpha: {}^{\circ}\text{K}^{-1}\\ \text{isothermal bulk modulus, } K_I: \text{GPa}: 10^9\ \text{kg}/(\text{m s}^2)\\ \text{adiabatic bulk modulus, } K_A: \text{GPa}\\ \text{specific heat, } c: \text{MPa}/{}^{\circ}\text{K}: 10^6\ \text{kg}/(\text{m s}^{2\,\circ}\text{K})\\ \text{thermal conductivity, } \gamma: \ \text{m kg}/(\text{s}^{3\,\circ}\text{K})\\ \text{thermal diffusivity } D' = \gamma/c: \ \text{m}^2/\text{s},\end{array} \tag{D.1}$$

where c and α here are ρc and $\alpha/3$ of Kjartansson, respectively, i.e., Kjartansson α is the volumetric thermal expansion.

Since [15]

$$K_A = K_I + \frac{\beta^2 T_0}{c}, \quad \text{and} \quad \beta = 3K_I\alpha,$$

we have

$$K_A = K_I\left(1 + \frac{9K_I\alpha^2 T_0}{c}\right) = K_I(1+\delta). \tag{D.2}$$

Eq. (5.36) of Kjartansson is

$$K_A = K_I\left(1 - \tfrac{9K_I\alpha^2 T_0}{c}\right)^{-1} \approx K_I\left(1 + \frac{9K_I\alpha^2 T_0}{c}\right),$$

since the 2nd term is small, unless for gas (steam and nitrogen). However, the values of δ [obtained with equation (D.2)] are slightly different from those of Table 5.2 of [7]. For steam and nitrogen, the values differ significantly.

From Table 1, we re-built another Table based on the parameters of the present paper.

Appendix E. Zener mechanical model

The Zener or standard-linear-solid model can be used to approximate the quality factor and phase velocity as a function of frequency. The complex modulus of the Zener model is

$$Z(f) = \frac{Q_0 + \mathrm{i}(f/f_0)(R+1)}{Q_0 + \mathrm{i}(f/f_0)(R-1)} \cdot Z_0, \quad R = \sqrt{1+Q_0^2}, \tag{E.1}$$

where f_0 is the relaxation frequency, Q_0 is the minimum quality factor at f_0, Z_0 is the zero-frequency modulus, f is the frequency and $\mathrm{i} = \sqrt{-1}$. The unrelaxed modulus ($f \to \infty$) is $Z_\infty = [(R+1)/(R-1)]Z_0$, and the following relations holds, $Q_0 = 2\sqrt{Z_\infty Z_0}/(Z_\infty - Z_0)$, so that the modulus dispersion $Z_\infty - Z_0$ can approximately be obtained from Q_0. Equation (E.1) has been obtained by [35] for a rod of arbitrary cross section vibrating transversely, where Z_0 and Z_∞ correspond to the isothermal and adiabatic moduli [[1, 36], Eq. (3.41)].

The Zener Q factor is [20]

$$Q = \frac{\mathrm{Re}(Z)}{\mathrm{Im}(Z)} = \frac{Q_0}{2} \cdot \frac{1 + (f/f_0)^2}{f/f_0}, \tag{E.2}$$

and the phase velocity is

$$c_p = \left[\mathrm{Re}\left\{\tfrac{1}{v}\right\}\right]^{-1}, \quad v = \sqrt{\frac{Z}{\rho}}, \tag{E.3}$$

where v is the complex velocity and ρ is the mass density [20].

Disclosure statement

No potential conflict of interest was reported by the authors.

Funding

This work was supported by the National Natural Science Foundation of China (grant no. 41974123 and 42174161), and the Jiangsu Natural Science Fund for Distinguished Young Scholars.

References

[1] C. Zener, "Internal friction in solids. II. General theory of thermoelastic internal friction," *Phys. Rev*, vol. 53, no. 1, pp. 90–99, 1938. DOI: 10.1103/PhysRev.53.90.
[2] B. H. Armstrong, "Models for thermoelastic in heterogeneous solids attenuation of waves," *Geophysics*, vol. 49, no. 7, pp. 1032–1040, 1984. DOI: 10.1190/1.1441718.
[3] Z. W. Wang, L. Y. Fu, J. Wei, W. T. Hou, J. Ba and J. M. Carcione, "On the Green function of the Lord-Shulman thermoelasticity equations," *Geophys. J. Int*, vol. 220, pp. 393–403, 2020. DOI: 10.1093/gji/ggz453.
[4] A. B. Jacquey, M. Cacace, G. Blöcher and M. Scheck-Wenderoth, "Numerical investigation of thermoelastic effects on fault slip tendency during injection and production of geothermal fluids," *Energy Proc.*, vol. 76, pp. 311–320, 2015. DOI: 10.1016/j.egypro.2015.07.868.
[5] R. J. Phillips and R. E. Grimm, "Martian seismicity, Lunar Planet," *Sci. Conf*, vol. XXII, Abstract 1061, pp. 13–14, 1991.
[6] E. Kjartansson, "Constant Q-wave propagation and attenuation," *J. Geophys. Res*, vol. 84, no. B9, pp. 4737–4748, 1979. DOI: 10.1029/JB084iB09p04737.
[7] E. Kjartansson, "Attenuation of seismic waves in rocks and applications in energy exploration," Ph.D. thesis, Stanford University, 1980.
[8] R. W. Zimmerman, "Coupling in poroelasticity and thermoelasticity," *Int. J. Rock Mech. Mining Sci.*, vol. 37, no. 1-2, pp. 79–87, 2000. DOI: 10.1016/S1365-1609(99)00094-5.
[9] M. A. Biot, "Thermoelasticity and irreversible thermodynamics," *J. Appl. Phys.*, vol. 27, no. 3, pp. 240–253, 1956. [Database] DOI: 10.1063/1.1722351.
[10] H. Lord and Y. Shulman, "A generalized dynamical theory of thermoelasticity," *J. Mech. Phys.*, vol. Solid 15, no. 5, pp. 299–309, 1967.
[11] J. C. Maxwell, "On the dynamic theory of gases, Phil. Trans," *Roy. Soc. London*, vol. 157, pp. 49–88, 1867.
[12] P. Vernotte, "Théorie continue et théorie moléculaire des phénomènes thermocinétiques," *C. R. Acad. Sci. (Paris)*, vol. 227, pp. 43–44, 1948.
[13] C. Cattaneo, "Sur une forme de l'équation de la chaleur éliminant paradoxe d'une propagation instantanée," *C. R. Acad. Sci. (Paris)*, vol. 247, pp. 431–433, 1958.
[14] A. J. Rudgers, "Analysis of thermoacoustic wave propagation in elastic media," *J. Acoust. Soc. Am*, vol. 88, no. 2, pp. 1078–1094, 1990. [Database] DOI: 10.1121/1.399856.
[15] J. M. Carcione, F. Cavallini, E. Wang, J. Ba and L.-Y. Fu, "Physics and simulation of wave propagation in linear thermo-poroelastic media," *J. Geophys. Res. Solid Earth*, vol. 124, no. 8, pp. 8147–8166, 2019a. DOI: 10.1029/2019JB017851.
[16] J. M. Carcione, Z.-W. Wang, W. Ling, E. Salusti, J. Ba and L.-Y. Fu, "Simulation of wave propagation in linear thermoelastic media," *Geophysics*, vol. 84, no. 1, pp. T1–T11, 2019b. DOI: 10.1190/geo2018-0448.1.
[17] J. Geertsma and D. C. Smit, "Some aspects of elastic waves propagation in fluid-saturated porous solids," *Geophysics*, vol. 26, no. 2, pp. 169–181, 1961. DOI: 10.1190/1.1438855.
[18] J. M. Carcione, "Viscoelastic effective rheologies for modeling wave propagation in porous media, Geophys," *Prosp*, vol. 46, pp. 249–270, 1998.
[19] J. E. White, N. G. Mikhaylova and F. M. Lyakhovitskiy, "Low-frequency seismic waves in fluid saturated layered rocks," *Izvestija Acad. Sci. USSR, Phys. Solid Earth*, vol. 11, pp. 654–659, 1975.
[20] J. M. Carcione. *Wave Fields in Real Media. Theory and Numerical Simulation of Wave Propagation in Anisotropic, Anelastic, Porous and Electromagnetic Media*, 3rd ed, (extended and revised). The Netherlands: Elsevier, 2014.
[21] J. Savage, "Thermoelastic attenuation of elastic waves by cracks," *J. Geophys. Res*, vol. 71, no. 16, pp. 3929–3938, 1966. Correction: 1967, JGR, 72, 6387. DOI: 10.1029/JZ071i016p03929.
[22] J. M. Carcione, D. Gei, J. E. Santos, L.-Y. Fu and J. Ba, "Canonical analytical solutions of wave-induced thermoelastic attenuation, Geophys," *J. Int.*, vol. 221, pp. 835–842, 2020a.
[23] L. D. Landau and E. M. Lifshitz, *Theory of Elasticity*. Oxford, England: Pergamon Press, 1970.
[24] J. Ignaczak and M. Ostoja-Starzewski, *Thermoelasticity with Finite Wave Speeds*. Oxford, England: Oxford University Press, 2010.
[25] E. Wang, J. M. Carcione, F. Cavallini, M. A. B. Botelho and J. Ba, "Generalized thermo-poroelasticity equations and wave simulation," *Surv Geophys*, vol. 42, no. 1, pp. 133–157, 2021. DOI: 10.1007/s10712-020-09619-z.
[26] A. E. Green and K. A. Lindsay, "Thermoelasticity," *J. Elasticity*, vol. 2, pp. 1–7, 1972.

[27] F. Gassmann, "Über die elastizität poröser medien," *Vierteljahresschrift der Naturforschenden Gesellschaft in Zurich*, vol. 96, pp. 1–23, 1951.
[28] M. Krief, J. Garat, J. Stellingwerff and J. Ventre, "A petrophysical interpretation using the velocities of P and S waves (full waveform sonic," *The log Analyst*, vol. 31, pp. 355–369, 1990.
[29] M. O'Donnell, E. T. Jaynes and J. G. Miller, "Kramers-Kronig relationship between ultrasonic-attenuation and phase-velocity," *J. Acoust. Soc. Am*, vol. 69, no. 3, pp. 696–701, 1981. DOI: 10.1121/1.385566.
[30] J. M. Carcione, F. Cavallini, J. Ba, W. Cheng and A. Qadrouh, "On the Kramers-Kronig relations," *Rheol. Acta*, vol. 58, pp. 21–28, 2018a. DOI: 10.1007/s00397-018-1119-3.
[31] J. M. Carcione, F. Poletto, B. Farina and C. Bellezza, "3D seismic modeling in geothermal reservoirs with a distribution of steam patch sizes, permeabilities and saturations, including ductility of the rock frame," *Phys. Earth Planetary Interiors*, vol. 279, pp. 67–78, 2018b. DOI: 10.1016/j.pepi.2018.03.004.
[32] J. M. Carcione, F. Mainardi, S. Picotti, L.-Y. Fu and J. Ba, "Thermoelasticity models and P-wave simulation based on the Cole-Cole model," *J. Thermal Stresses*, vol. 43, pp. 512–527, 2020. DOI: 10.1080/01495739.2020.1722772.
[33] J. M. Carcione and F. Mainardi, "On the relation between sources and initial conditions for the wave and diffusion equations," *Comput. Math. Appl.*, vol. 73, no. 6, pp. 906–913, 2017. DOI: 10.1016/j.camwa.2016.04.019.
[34] D. F. Griffiths, J. W. Dold and D. J. Silvester, "Essential partial differential equations," in *Analytical and Computational Aspects*. Berlin: Springer, 2015.
[35] C. Zener, "Internal friction in solids. I. Theory internal friction," *Phys. Rev*, vol. 52, pp. 230–235, 1937.
[36] F. Mainardi, *Fractional Calculus and Waves in Linear Viscoelasticity*. Singapore: Imperial College Press, 2010.